Absence of chaos in a self-organized critical coupled map lattice

Ákos Csilling,[1] Imre M. Jánosi,[2,*,†] Gabriella Pásztor,[1] and István Scheuring[3]
[1]*Department of Atomic Physics, Eötvös University, Budapest, Puskin utca 5-7, H-1088, Hungary*
[2]*Theoretical Physics, FB 10, University of Duisburg, D-47048 Duisburg, Germany*
[3]*Department of Plant Taxonomy and Ecology, Mathematical Modelling Group, Eötvös University, Budapest, Ludovika tér 2, H-1081, Hungary*
(Received 31 January 1994)

Although ecologists have been aware for almost 20 years that population densities may evolve in a chaotic way, the evidence for chaos in *natural* populations is rather poor. The lack of convincing evidence may have its origin in the difficulty of estimating the effect of external environmental noise, but it may also reflect natural regulation processes. In this paper we present a meta-population-dynamical model, in which the nearest neighbor local population fragments interact by applying a threshold condition. Namely, each local population follows its own temporal evolution until a critical population density is reached, which initiates dispersal (migration) events to the neighbors. The type of interaction is common to self-organized critical cellular automaton models. Depending on the threshold level, the global behavior of our model can be characterized either by noisy dynamics with many degrees of freedom, by a periodical evolution, or by an evolution towards a fixed point. Low dimensional collective chaos does not occur. Moreover, self-organized criticality with power law distributions emerges if the interaction between the neighboring local populations is strong enough.

PACS number(s): 05.40.+j, 05.45.+b, 05.70.Jk

I. INTRODUCTION

An important unsolved problem of population biology is that natural populations usually do not evolve in a chaotic way [1–6], whereas theoretical models and laboratory experiments frequently predict such a behavior. The reason for this disagreement may lie in additional self-regulating mechanisms in natural populations. On the other hand, a recent theory dubbed "self-organized criticality" (SOC) [7] provides a unifying concept for large scale behavior in systems with many interactive degrees of freedom. This phenomenon is expected to be quite universal and it has been looked for in such diverse areas as geophysics, economics, condensed matter physics, and astrophysics. In this article we present an alternative population-dynamical model which exhibits self-organized criticality and shows nonchaotic global behavior.

A common basic assumption in population-dynamical models is that populations are uniformly dispersed in the habitats [8,9], and the relevant variable, the population density, can be described by ordinary differential or difference equation [8,10,12]. If spatial heterogeneity is taken into account, it is convenient to model the dynamics by transport-reaction processes [9,10]. Although these models may give a satisfactory description of local populations, they oversimplify the effect of spatial heterogeneity in many cases.

It is better to consider the so called metapopulation, which is built up by local populations living in habitat fragments and individuals dispersed among these local habitats [11]. Many studies of metapopulations have concentrated on the occupation and extinction in local habitats and frequently have allowed only two values for the local population density [13,14]. The crucial problem in these models is to implement a realistic mechanism for the dispersal. The simplest idealization is to assume that the rate of dispersion does not depend on the density and the distance between habitat fragments [13]. Other models take into account either the density [14,15] or distance [16] dependences, but usually in a continuous way.

Our model takes into account the density *and* distance dependences via a threshold condition, which is common in SOC models and biologically well confirmed. The first assumption is that migrations are enabled only among the nearest neighbor local habitat fragments. This does not exclude the possibility that a local dispersal could affect a more distant local population by a series of elementary steps. Although this assumption is too strict in the case of terrestrial vertebrates, it is appropriate for many insects [17]. The second basic assumption is that a migration event is triggered by the overcrowding of a local population and its size depends on the local density, in agreement with several observations [17,18].

II. MODEL

Consider a set of $L \times L$ sites on a two-dimensional square lattice representing local habitat fragments. To each site (i,j) we assigned a continuous variable $N_{i,j}$,

*Author to whom correspondence should be addressed.
†Permanent address: Department of Atomic Physics, Eötvös University, Puskin utca 5-7, H-1088 Budapest, Hungary.

which characterizes the local population density. The main difference from the other SOC models [19] is that each site has its own time evolution according to the following well known discretized differential equation, which is widely used to model the time evolution of a local population [1]:

$$N_{i,j}(t+1) = \lambda N_{i,j}(t)[1 + aN_{i,j}(t)]^{-\beta}. \quad (1)$$

Here λ denotes the intrinsic growth rate parameter, a is a scaling parameter, the exponent β describes the density dependence, and the discrete time t represents, e.g., the time of annual censuses. Depending on the values of λ and β, there exist a fixed point, stable limit cycles, in which the population alternates up and down, or chaos; the scaling parameter a does not affect the stability properties [1,10].

A dispersal event (migration) occurs if the population density at a site exceeds some prescribed critical value $k_{i,j}$ (for the sake of simplicity we can use a uniform critical value $k = k_{i,j}$ for all i,j). We use the following elementary migration rule:

$$N_{i,j} \longrightarrow N_{sc}, \quad (2a)$$

$$N_{i\pm1,j\pm1} \longrightarrow N_{i\pm1,j\pm1} + \Delta\frac{N_{i,j} - N_{sc}}{4}, \quad (2b)$$

where N_{sc} denotes the (uniform) subcritical population density at which the dispersal ceases ($N_{sc} < k$) and Δ is a dissipation parameter representing, e.g., a decrease of the population during the migrations ($0 < \Delta \leq 1$). In the following we restrict ourselves to the conserving case $\Delta = 1$. Since the migrated population increases the density at the neighboring sites, further activation events may occur. A local dispersal event may trigger activation on a set of connected sites, resulting in a "migration avalanche." The boundaries are open in the sense that population fragments reaching the boundary sites will leave the system freely (or disappear).

The system evolves in the following way. We start from a random initial configuration and all sites are simultaneously updated according to Eq. (1). When on one or more sites the state variable $N_{i,j}$ exceeds the threshold value k, the time evolution stops, and relaxation processes according to Eq. (2) begin, until every site becomes subcritical. In other words, we consider the dispersal as instantaneous and do not allow for time evolution during migrations.

Note that rule (2) obeys a local conservation law during the migration in the case of $\Delta = 1$; however, the model is globally nonconservative because the population at a given site can decrease spontaneously according to the time evolution rule (1).

It is easy to recognize that this model is a special case of coupled map lattices (CMLs). A CML is a dynamical system with a discrete time, discrete space, and continuous state variables exhibiting very complex collective behavior known as spatiotemporal chaos [20]. The most widely investigated CML is the diffusively coupled logistic map array. In two dimensions it is given by

$$y_{i,j}(t+1) = (1-\epsilon)f(y_{i,j}(t)) + \frac{\epsilon}{4}\sum_{k,l\in nn} f(y_{k,l}(t)), \quad (3)$$

where $y_{i,j}$ is the continuous state variable, t is the discrete time, ϵ denotes the coupling parameter, and the summation runs over the nearest neighborhood of the site (i,j). The mapping function $f(y)$ is the well known logistic map

$$f(y) = \lambda y(1-y) \quad (4)$$

with the control parameter λ. The simplicity of this map is very attractive; however, in practical applications Eq. (4) has the disadvantage that it requires y to remain within the interval $0 < y < 1$ to avoid the divergence to minus infinity. Therefore, the map (1) was chosen for our model, which has finite solutions on the whole domain of positive real numbers. Apart from the generating map, there are two main differences between our model and diffusively coupled CMLs. First, the coupling in our model obeys a threshold condition; however, the relaxation mechanism above the threshold is also diffusive. Second, there exists a time scale separation in our model as mentioned above: During the relaxation processes the global time evolution stops.

III. GENERAL BEHAVIOR AND SCALING PROPERTIES

In this article we mainly concentrate on the effect of threshold dynamics on the chaotic behavior of the metapopulation density. The parameters of Eq. (1) were chosen to be initially $\lambda = 100.0$, $a = 1.0$, and $\beta = 8.8$. We stress here that these parameters belong to the strong chaotic domain [1] of Eq. (1). The other parameters, namely, the system size L and the subcritical value of the state variable N_{sc}, were found not to be relevant for the global behavior. We will discuss their effects further below. The only important parameter that remains is the threshold level k initiating the dispersal processes.

First, we discuss the temporal behavior of a local population (a single site) and of the metapopulation (the whole lattice). In Fig. 1 we have plotted the time series, the first return maps, and the power spectra of the population density $N_{i,j}(t)$ of a single site ($i = j = 8$ on a lattice of 16×16), with different threshold levels. Figures 1(a1)–1(a3) show the characteristics of Eq. (1), which corresponds to the $k = \infty$ limit, when there is no migration in the system. The following rows [Figs. 1(b)–1(e)] represent the effect of increasing interaction (decreasing threshold level). The chaotic nature of the local dynamics, generated by the governing equation Eq. (1), tends to be suppressed as the interaction increases, until it reaches a (noisy) fixed point [see Figs. 1(e)]. [Note the different scale in Fig. 1(e2)]. It can be seen as well that the increasing interaction results in the appearance of some discrete peaks in the power spectra [Figs. 1(b3)–1(d3)], which reflects the emergence of periodic behavior,

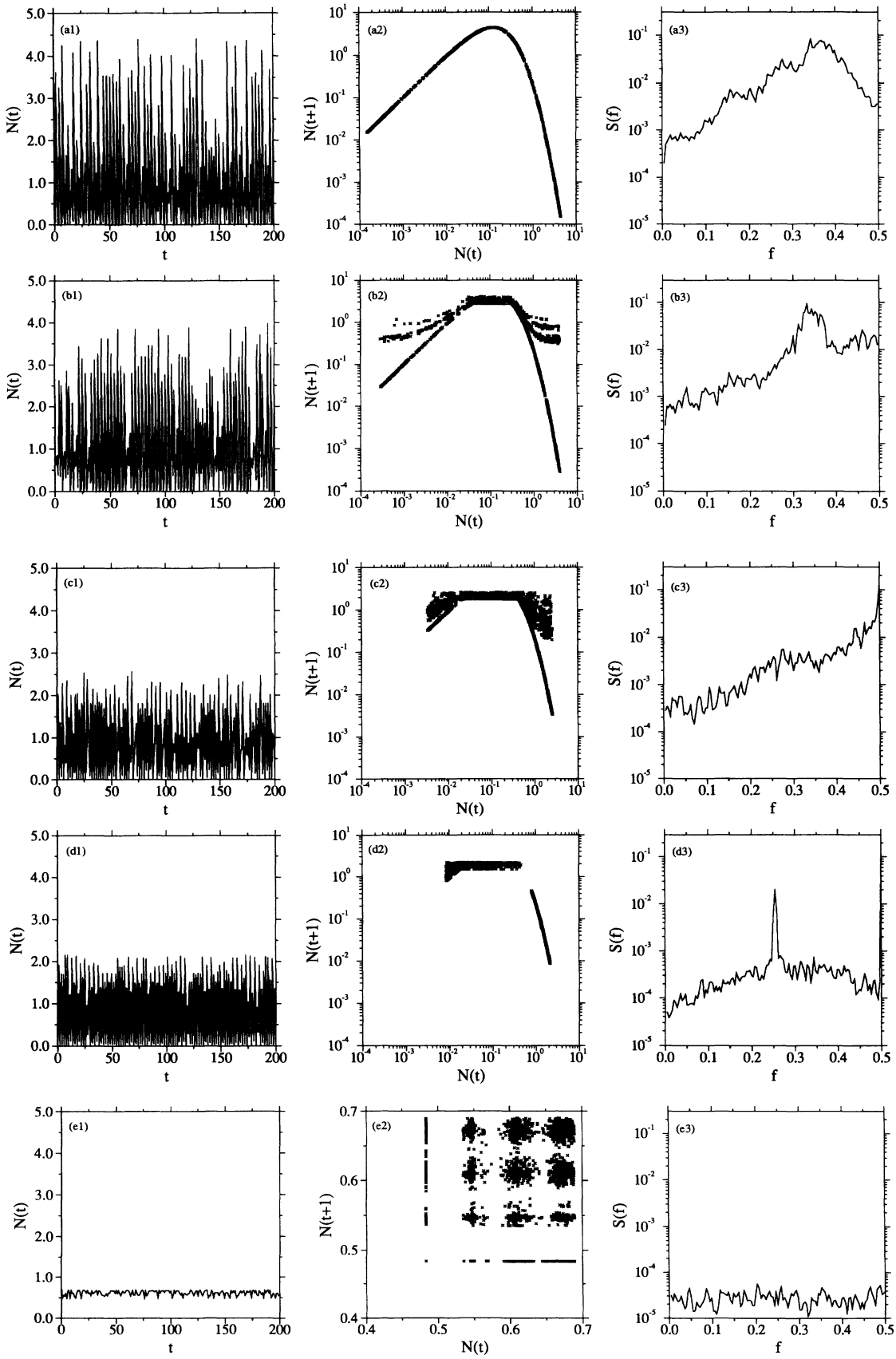

FIG. 1. Time series, first return maps, and power spectra of the population density N of a given site with varying threshold parameter. (a) No interaction ($k = \infty$), (b) $k = 4.0$, (c) $k = 2.69$, (d) $k = 2.165$, and (e) $k = 0.69$ (from top to bottom).

while at the final fixed point white noise with a very small amplitude remains [Fig. 1(e3)].

Figure 2 demonstrates the same characteristics as Fig. 1, but it refers to lattice averages:

$$\langle N(t)\rangle = \frac{1}{L^2}\sum_{i,j} N_{i,j}(t). \tag{5}$$

As before, the averages were measured after finishing all dispersal events. The first row [Figs. 2(a1)–2(a3)] refers again to the noninteractive case. The time series data [Figs. 2(a1)–2(e1)] are plotted from a random initial configuration (t=0). Note that the steady state is reached very fast in all cases. The return map [Fig. 2(a2)] does not indicate low dimensional chaos, as it is a trivial consequence of the many independent degrees of freedom entering the lattice average. As intuitively expected, the increasing interaction strength suppresses the noisy dynamics and the collective behavior becomes more and more pronounced. This is reflected by the increased correlations visible in the return maps [Figs. 2(b2)–2(c2)] and the appearance of discrete frequencies in the power spectra (Figs. 2(b3)–2(c3)]. When the threshold level is small enough, the time evolution is strictly periodic [Figs. 2(d2)–2(d3)] or shows a stable fixed point equilibrium (Figs. 2(e2)–2(e3)]. We have not been able to find any threshold value at which the collective dynamics shows low dimensional chaos.

It is interesting that there is no sign of spatial organization, even when the system settled down to a strictly periodic oscillatory state. To illustrate this fact, we plotted in Fig. 3 the space amplitude of a single row in a system of size $L = 35$. Figure 3(a) shows a segment of the time evolution of the lattice average at two different threshold values; the perfect periodicity is clearly visible. Figures 3(b) and 3(c) show the values of the state variable of the sites situated in the 16th row, $N_{i,16}$. Twenty consecutive time steps are plotted within each figure. While the alternating motion between a high and low level state is pronounced, there is no correlation between the values of neighboring sites, apart from the fact that they are bounded in two nonoverlapping intervals.

We note that this collective periodic behavior is completely different from the well-known collective periodic motion of the globally coupled oscillator arrays [21,22]. In our case the perfect oscillation is observable in the lattice average only, while the globally coupled nonlinear oscillator arrays obey perfect synchronization, i.e., every degree of freedom behaves in the same way as the lattice average.

This observation together with the following one have a close resemblance to a phenomenon dubbed "spontaneous noise reduction." Here we refer again to Figs. 1(d1)–1(d3) and Figs. 2(d1)–2(d3). It is obvious that while the time evolution of the state variable of a single site (at the given threshold value $k = 2.169$) obeys a period-4 cyclic motion with a wide-band backround noise, the evolution of the spatial average is perfectly smooth with an undetectable low noise background. A similar observation was mentioned [23] at an investigation of a resistively shunted Josephson-junction series array biased by an external current source. In that system the noise measured on the whole system has a considerably lower amplitude than that measured on a single junction. However, the average signal in that case is constant instead of oscillatory. This is perhaps not too surprising from a physical perspective, since the junctions are coupled to each other globally, so that one expects averaging effects due to the presence of the other junctions. The noise-reduction phenomenon is more surprising in our system because the system has only nearest neighbor coupling. This is the first sign that the relaxation process defined in our model may build up long range correlations.

One of the basic fingerprints of self-organized criticality is the power law behavior of the density function of the avalanche size distribution. Our system is globally driven, i.e., all sites evolve simultaneously. Thus, at a given time step several sites can become overcrowded, so that several migration avalanches can originate and interfere with others causing difficulties in obtaining the size distribution. Therefore, we have applied the local perturbation method [7] to obtain the avalanche-size statistics. First, the system is allowed to relax to a subcritical state ($N_{i,j} < k$ for all i,j); then a given site is locally perturbed by a small positive increment N'. This can cause a local migration step if $N_{i,j} + N' > k$, and the perturbation spreads over several neighboring sites according to the applied dynamical rules. The size s of the migration avalanche is defined by the total number of elementary dispersal steps induced by the single perturbation. After each perturbation, the original state is restored and another site is perturbed, etc. It is clear that the result depends on the size of the applied perturbation N'. Our numerical investigations show that a particular choice of N' affects exclusively the amplitude of the distribution functions and not the overall shape, however, too small values of N' result in poor statistics.

We think that the application of the local perturbation method is a technical question only. Since the model is non-Abelian [24], because the redistribution of the state variable is proportional to the instantaneous value in the relaxing site, then the temporal order of the elementary relaxation steps should be strictly followed. However, simultaneously occurring, colliding avalanches are not able to block each other as a result of the local conservation of the migrating population. Thus the shape of the obtained distribution functions must not be only an artifact of the measuring method.

In Fig. 4(a) the migration avalanche-size distribution densities are plotted for different threshold values. At the highest threshold level ($k \approx 4.0$) the distribution function can be fitted by an exponential function

$$P(s) \sim \exp\left(-\frac{s}{s^*}\right), \tag{6}$$

with a characteristical length $s^* = 1.00 \pm 0.08$. This refers to completely uncorrelated avalanches; moreover the interaction is restricted to nearest neighbors. In the intermediate range $2.7 \gtrsim k \gtrsim 2.3$, the distribution functions become more and more similar to a power law; however,

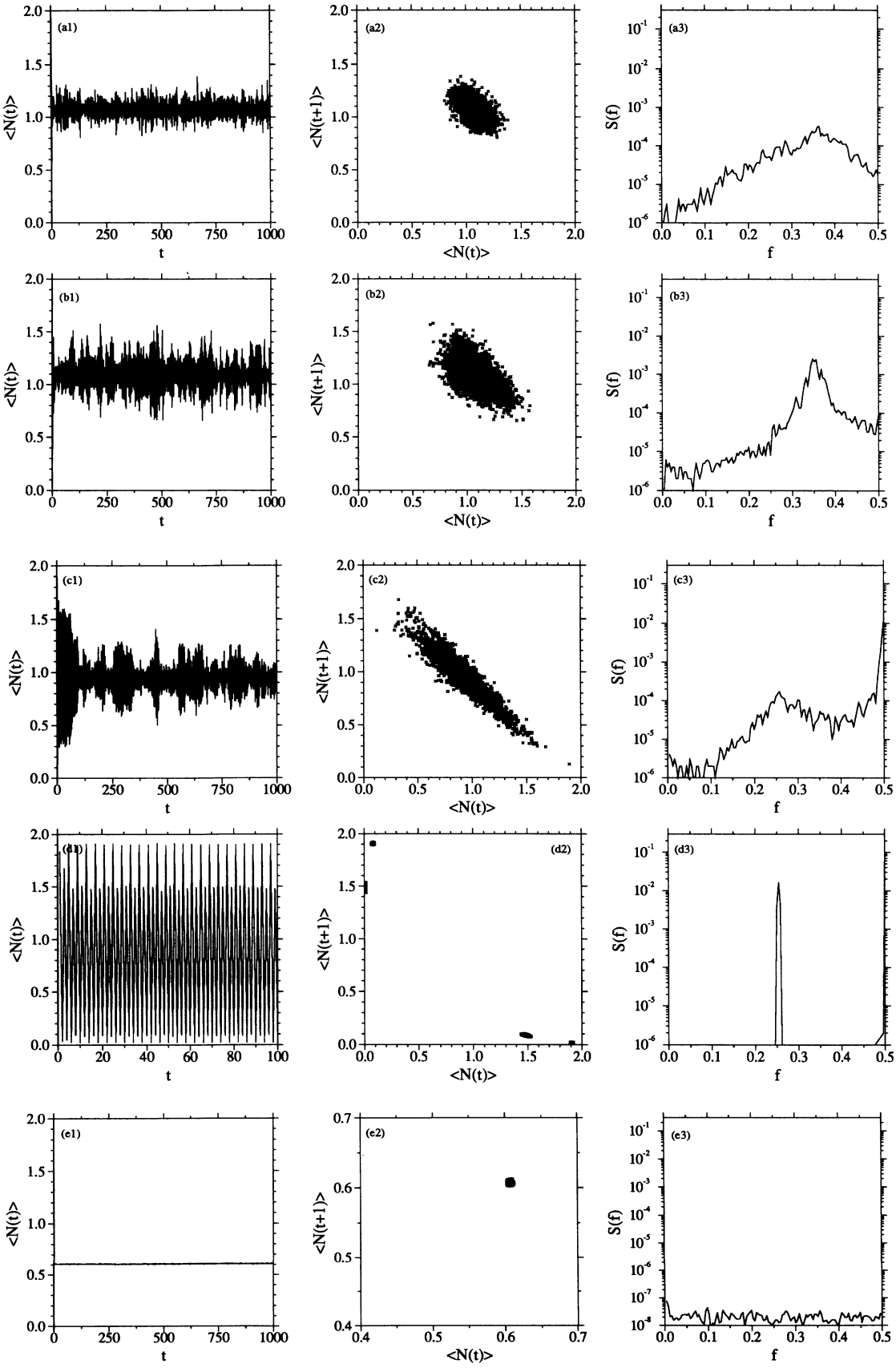

FIG. 2. Time series, first return maps, and power spectra of the metapopulation density [Eq. (5)] with varying threshold parameter. (a) No interaction ($k = \infty$), (b) $k = 4.0$, (c) $k = 2.69$, (d) $k = 2.165$, and (e) $k = 0.69$ (from top to bottom).

they are slightly bent in the double logarithmic plot. The fitting form

$$P(s) \sim s^{-\tau'} \exp\left(-\frac{s}{s'}\right) \tag{7}$$

gives very good result for these curves with an exponent values $1.0 \leq \tau' \leq 1.3$ and a "correlation length" $3.0 < s' < +\infty$ (s' diverges extremely fast when the threshold value is decreased). Finally, at low thresholds low ($k < 2.2$) pronounced power law shapes are observable:

$$P(s) \sim s^{-\tau}, \tag{8}$$

with $\tau = 1.20 \pm 0.08$, slightly depending on k. These power law shapes are significant for the buildup of long range correlations and the emergence of self-organized criticality.

To establish the critical state in a more convincing way, the scaling properties of the system are investigated by finite-size-scaling analysis [25]. Let $P(s, L)$ denote the distribution function in a system of linear size L. We use the finite-size-scaling ansatz

$$P(s, L) \sim L^{-\kappa} g\left(\frac{s}{L^{\nu}}\right), \tag{9}$$

where g is a universal scaling function, ν denotes the critical exponent which describes how the cutoff size scales with the system size, and κ is the exponent connected to the norm of the distribution functions. Moreover, if Eq. (8) holds, i.e., if the scaling function g obeys a power law with exponent τ, a scaling relation between the three critical indices exists [25]:

$$\tau = \frac{\kappa}{\nu}. \tag{10}$$

Figure 4(b) shows the results of the finite-size scaling analysis. The distribution functions for different lattice sizes collapse onto a universal form exhibiting the scaling relation (10) with the exponent values $\tau = 1.21 \pm 0.05$, $\kappa = 3.16 \pm 0.05$, and $\nu = 2.60 \pm 0.07$.

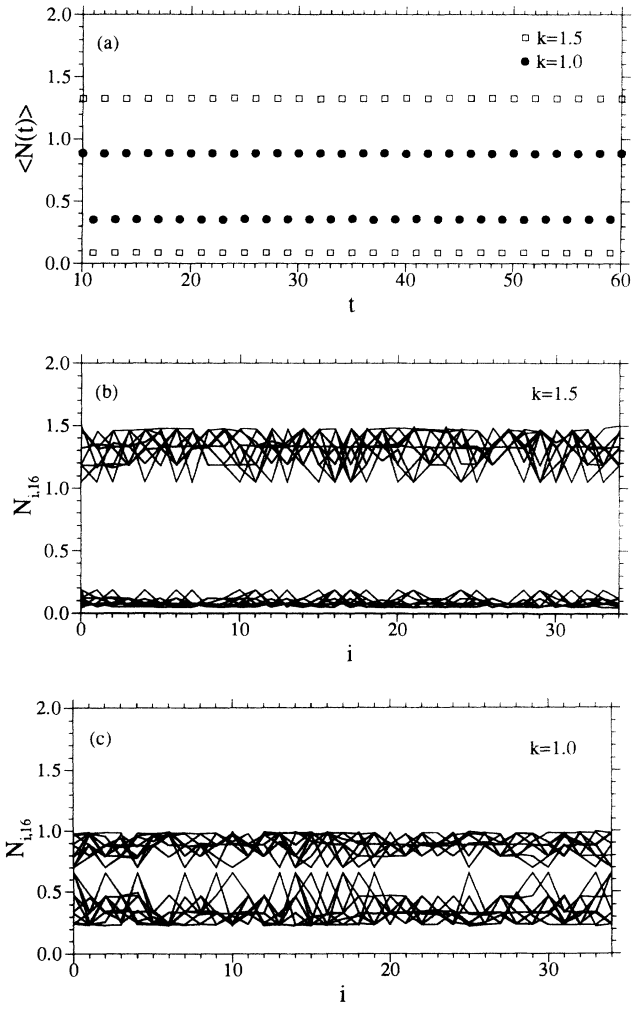

FIG. 3. (a) Time evolution of the lattice average in a system of size $L = 35$ at two threshold values. Space-amplitude plot of the 16th column for (b) $k = 1.5$ and (c) for $k = 1.0$, 20 consecutive time steps are plotted.

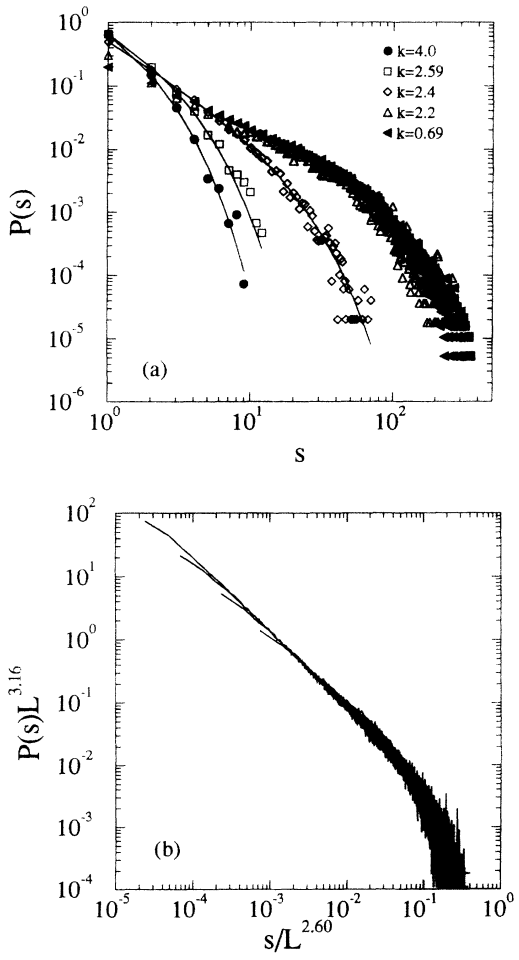

FIG. 4. (a) Migration avalanche-size distributions for a lattice of $L = 16$ with varying threshold parameters. (b) Finite size scaling analysis [Eq. (9)] at the threshold $k = 0.69$ for system sizes $L = 16,25,40,60$.

IV. CHANCE OF LOW DIMENSIONAL COLLECTIVE CHAOS

This section is devoted to the following question: What is the chance of observing low dimensional global chaos in our system at all? At the beginning of our analysis, we recall Grinstein's elegant reasoning [26] why generically a collective chaotic state in a broad class of extended many-body systems with short range interaction does not occur.

Let us imagine a general dynamic many-body system (such as coupled maps, cellular automata, or partial differential equations) characterized by scalar variables $x(\vec{r},t)$, which take on real values confined to the interval $0 \le x(\vec{r},t) \le x_{\max}$. The system evolves according to some dynamical rule [e.g., Eq. (1) or (4)], which is assumed to be deterministic and local. Imagine that a particular variable $x(\vec{r}_0,t)$ is perturbed by an infinitesimal amount ϵ at some time $t=0$ and then allowed to evolve without further external interference. If the system is in the chaotic regime, then the perturbed trajectory will diverge exponentially in time:

$$\Delta x(\vec{r}_0,t) \sim \epsilon \exp(\gamma t), \tag{11}$$

where Δx denotes the difference between the perturbed and unperturbed trajectories and γ is some positive Lyapunov exponent [27]. When t becomes so large that Δx is of the order of the allowed range $x_{\max}$, i.e.,

$$t \sim t^* = \frac{1}{\gamma} \ln\left(\frac{x_{\max}}{\epsilon}\right), \tag{12}$$

$x(\vec{r}_0,t)$ has been completely "dephased" by the perturbation, there is no way to estimate the initial value at $t=0$. The locality of the dynamics implies that information about the value of $x(\vec{r}_0,t)$ cannot spread to other parts of the system faster than with a given velocity v (in a usual cellular automaton with nearest neighbor couplings this velocity is one lattice spacing per time step). This defines a "coherence length" ξ in the system

$$\xi = vt^* = \frac{v}{\gamma} \ln\left(\frac{x_{\max}}{\epsilon}\right). \tag{13}$$

Variables at $\vec{r}$ with $|\vec{r}-\vec{r}_0| > \xi$ are not affected by the value of $x(\vec{r}_0,t)$. A finite spatial coherence length in locally chaotic systems implies the nonexistence of collective chaos under generic conditions. Naively one would expect that the incoherent averages over many essentially uncorrelated regions of linear size ξ show only stationary time independent behavior. This is often the case [see Fig. 2(a)]; however, Bohr *et al.* pointed out [28] that if the individual variables move periodically between chaotic bands, then the incoherent averages can produce a periodic time evolution reflecting the regular periodic motion between the bands.

The above result seems to be in contradiction with several experiments where low dimensional chaos were observed in macroscopic systems. However, one should stress that the chaotic behavior averaged away completely only in the thermodynamical limit. Obviously when ξ in Eq. (13) is comparable to or larger than the system size L, the system may behave chaotically even on its largest length scale. The regime $\xi \gtrsim L$ is easily achieved in practice: One possibility is to shrink the system size, the other is to tune the governing dynamics just above the onset of chaos, where the Lyapunov exponent has a very small positive value. In this case ξ diverges to infinity; see Eq. (13). Here we repeat again that colliding avalanches do not destroy each other; thus avalanche overlapping cannot decrease drastically the coherence length ξ. We have tried both methods mentioned above with the following results.

First, the parameters were not changed except the lattice size. Figure 5 shows the effects of a gradually decreasing threshold in a system of size $L=3$. This is the smallest possible system which contains not only boundary sites. When the coupling is weak, the center site does not feel the neighbors at all [Fig. 5(a1)], the lattice average [Fig. 5(a2)] shows uncorrelated noise. When the coupling is increased, the arms of the first return map appear [Fig. 5(b1)], while the average remains almost completely uncorrelated [Fig. 5(b2)]. Decreasing further the threshold, the system abruptly settles down to a period-4 motion; however, this motion is not synchronized [Figs. 5(c1) and 5(c2)], i.e., the cycles of the different sites are different from each other and from the average. An important difference from the behavior of the large systems is that the configurations of this period-4 motion are spatially organized into symmetric patterns, i.e., the time evolution is realized within the periodic change between four patterns. Note that the difference of the threshold values between the cases of Figs. 5(b) and 5(c) is extremely low ($\Delta k = 0.000\,000\,5$). Furthermore the heavy dots in Fig. 5(c) are not the consequence of some noise or scatter of data, but only for the ease of visualization.

The crossover point, where the perfect oscillation appears, does not have universal characteristics. The threshold value depends slightly on the dynamical parameters λ and β and on the parameter of the relaxation rule N_{sc} as well. However, the extremely abrupt appearance of the perfect oscillation can be considered as a generic behavior at such a small system size. In larger systems, the transition from the noisy collective state to the oscillatory state is smeared out: The larger the size, the wider the transition regime; however, it is difficult to characterize this transition quantitatively.

The other method in order to enlarge the coherence length ξ is the decrease of the Lyapunov exponent. The dependence of the Lyapunov exponent on the dynamical parameter β [see Eq. (1)] is plotted in Fig. 6, which was obtained by a standard method [29]. At our earlier simulations, the parameter β was changed in a narrow interval around the value $\beta = 8.8$, the Lyapunov exponent has a value $\gamma = 0.44 \pm 0.01$ in this regime. To check the effect of a small Lyapunov exponent, we then fixed the value at $\beta = 7.275$, corresponding to $\gamma = 0.0230 \pm 0.0005$, and kept the system size at $L=3$. In this case, the crossover from the noisy behavior to the perfect oscillation is smeared out similarly to the behavior of large systems; however, important differences exist. In Fig. 7(a)

the first return map of the lattice average is plotted at an intermediate k value in the transient regime. The apparent low dimensional structure suggests that this motion exhibits low dimensional collective chaos. In Fig. 7(b) the same return map is plotted in a double logarithmic scale together with the solution of Eq. (1) at the same parameter values. This illustrates that the attractor of the collective behavior is completely different from the noninteracting case. In Fig. 8(a) the time series of the middle site is plotted for the same system, while Fig. 8(b) shows the time evolution of the lattice average resulting in the first return map of Fig. 7. Careful investigations show that the motion represented by the first return map is not chaotic in the strict sense. The power spectrum of the average corresponds to a global peridod-2 motion with a wide-band noisy background and there is no detectable positive Lyapunov exponent. The source of this noise is incoherent intermittent bursts in the single site dynamics [Fig. 8(a)], which are almost perfectly oscillatory. This interesting behavior shows an alternative aspect of the extremely rich collective dynamics of this model.

V. DISCUSSION

We have demonstrated that the global metapopulation does not show collective chaotic behavior if local habitats interact via the threshold rule common in SOC models. In a wide parameter range the dynamic behavior is either noisy (with many degrees of freedom), periodic, or converges to a stable fixed point. The absence of collective chaos is not trivial, especially at small system sizes, because the criticality of the model results in an infinite coherence length. Furthermore, because of the time scale separation the signal propagation speed is infinite as well. However, this statement is valid only "occasionally" because the interaction is switched on above a threshold exclusively. Thus we believe that this threshold condition

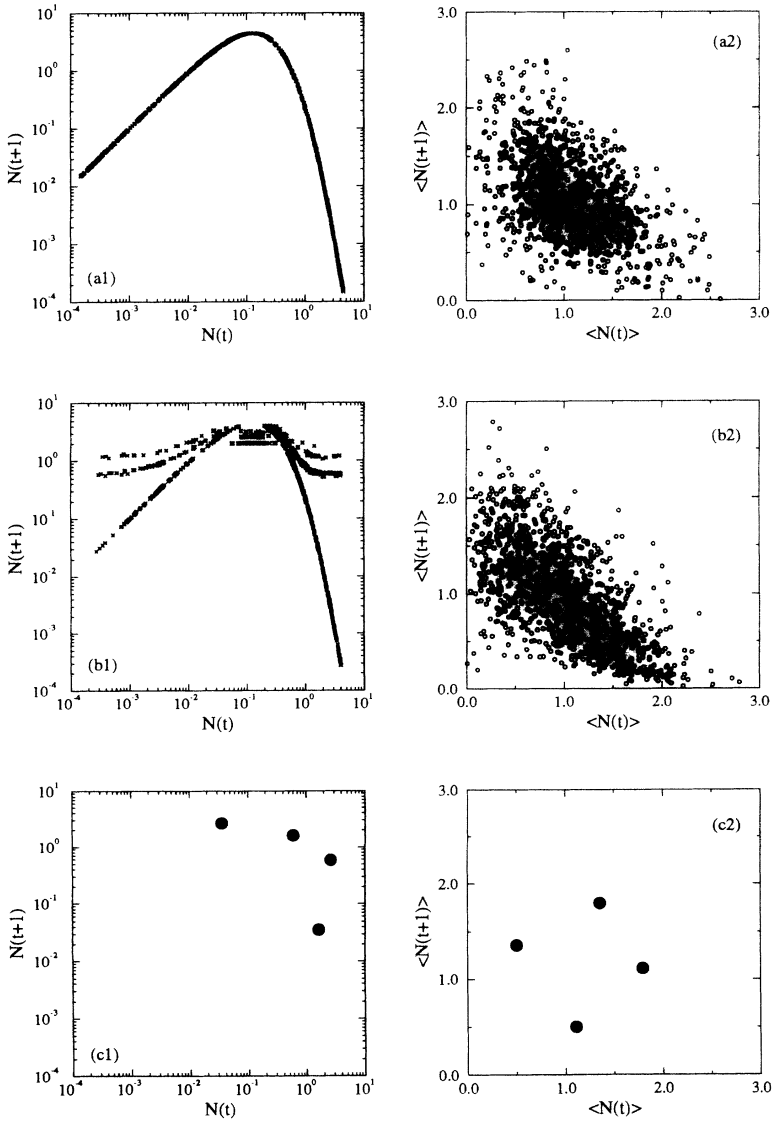

FIG. 5. First return map of the time series of the central site (left column) and the lattice average (right column) for a system of size $L = 3$. The threshold values are (a) $k = 3.20$, (b) $k = 3.046\,695\,5$, and (c) $k = 3.046\,696\,0$.

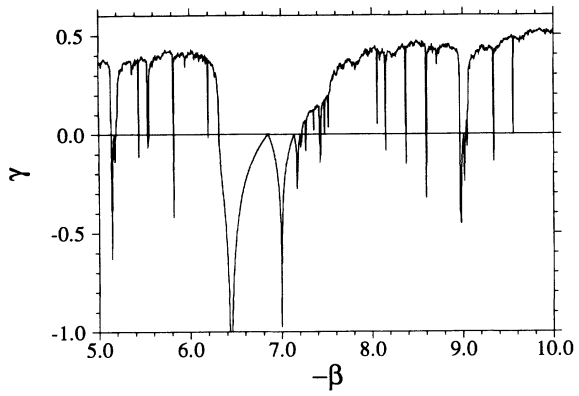

FIG. 6. Dependence of the Lyapunov exponent on the parameter β [see Eq. (1)]. The spectrum was obtained by averaging the Jacobian of the map Eq. (1) over 10 000 iterations for every fixed value of β.

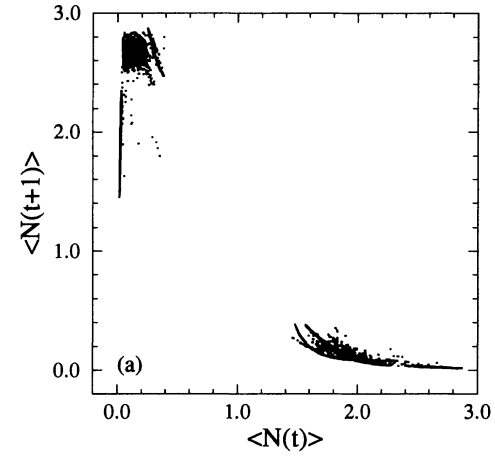

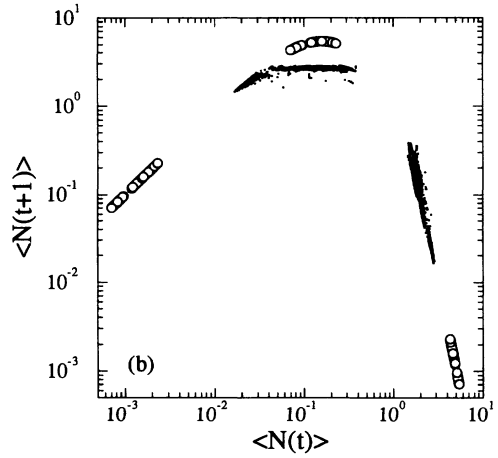

FIG. 7. (a) First return map of the time series of the lattice average for a system of size $L = 3$ and parameter values $\lambda = 100.0$, $a = 1.0$, $\beta = 7.275$, and $k = 3.150$. (b) The same as (a) in a double logarithmic plot together with the attractor of a noninteracting site (opaque circles).

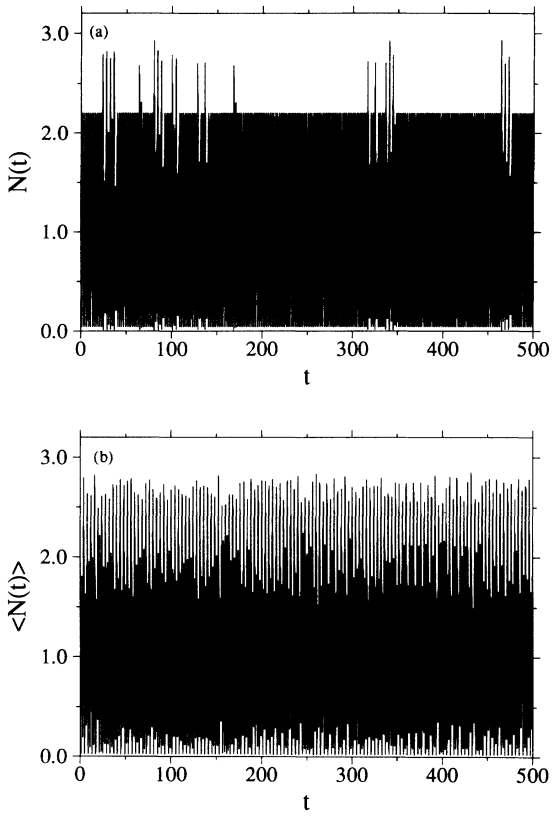

FIG. 8. Time series of (a) the central site and (b) the lattice average for the same parameters as in Fig. 7.

inhibits the buildup of collective chaos: The dynamics of a single site is not influenced permanently by its environment so that dephasing occurs below the threshold.

It is easier to understand the buildup of almost perfect oscillatory collective states. An important characteristic of the relaxation rule used in this model is the presence of a very robust self-averaging process [30,31]. After a relaxation cycle the distribution of the state variable is sharply peaked around the multiples of a characteristic value. If the coupling is strong enough, i.e., the threshold is low enough, the relaxed configuration can by described by a few discrete density values, which do not depend on the initial configuration. Thus all sites will evolve more or less coherently in time. This finally leads to a collective behavior characterized by cyclic occurrences of some more or less frozen patterns.

This model is an interesting type of SOC cellular automaton model. While the avalanche-size distribution shows a power law behavior which is the main characteristic of SOC, the power spectrum of the time series differs markedly from the usual broadband colored noise. We have observed white or spiky power spectra in contrast to the typical $1/f^2$ behavior [32] of the other SOC models.

The simulational results agree well with the overwhelming part of field observations, where only in some exceptional cases a partially chaotic time evolution was

found [33]. We note again that most populations, which showed more or less convincing evidence for chaotic behavior, were observed in laboratory experiments, i.e., in populations isolated from any environmental interaction. The biological relevance of our model could be checked by a statistical analysis of some real migration data, i.e., through the comparison of their avalanche-size statistics with the results of our simulations.

ACKNOWLEDGMENTS

We would like to thank Dietrich Wolf for illuminating discussions and Martin Siegert for careful reading of the manuscript. The research was supported by the Hungarian National Science Foundation (OTKA) under Grant No. 2091, and by the PHARE ACCORD Program (OMFB) No. H9112-0395.

[1] M. P. Hassel, J. H. Lawton, and R. M. May, J. Anim. Ecol. **45**, 471 (1976).
[2] W. M. Schaffer and M. Kot, J. Theor. Biol. **112**, 403 (1985).
[3] P. Turchin, Nature **344**, 660 (1990).
[4] G. J. Witteman, A. Readfearn, and S. L. Pimm, Evol. Ecol. **4**, 173 (1990).
[5] P. Turchin, J. Anim. Ecol. **60**, 1091 (1991).
[6] H. C. J. Godfray and B. T. Grenfell, Trends Ecol. Evol. **8**, 43 (1993).
[7] P. Bak, C. Tang, and K. Wiesenfeld, Phys. Rev. Lett. **59**, 381 (1987); Phys. Rev. A **38**, 364 (1989).
[8] C. J. Krebs, *The Experimental Analysis of Distribution and Abundance*, 3rd ed. (Harper & Row, New York, 1985).
[9] *Mathematical Ecology: An Introduction*, edited by T. G. Hallam, S. A. Levin (Springer-Verlag, Berlin, 1986).
[10] *Theoretical Ecology: Principles and Applications*, 2nd ed., edited by R. M. May (Blackwell, Oxford, 1981).
[11] S. Wright, Am. Nat. **74**, 232 (1940).
[12] *Individuals, Populations and Communities*, edited by M. Begon, J. Harper, and C. R. Townsend (Blackwell, Oxford, 1986).
[13] R. Levins, in *Some Mathematical Problems in Biology*, edited by M. Gerstenhaber (American Mathematical Society, Providence, RI, 1970), p. 77.
[14] I. Hanski and M. Gilpin, Biol. J. Linnean Soc. **42**, 3 (1991).
[15] M. Gadgil, Ecology **52**, 253 (1971).
[16] R. H. MacArthur and E. O. Wilson, *The Theory of Island Biogeography* (Princeton University Press, Princeton, 1967).
[17] L. Hansson, Biol. J. Linnean Soc. **42**, 89 (1991), and references therein.
[18] I. Hansky, Ecology **66**, 335 (1985).
[19] I. M. Jánosi, Ph. D. thesis, Eötvös University, 1992.
[20] K. Kaneko, in *Formation, Dynamics and Statistics of Pattern - Vol. 1*, edited by K. Kawasaki, A. Onuki, and M. Suzuki (World Scientific, Singapore, 1990), p. 1.
[21] R. E. Mirollo and S. H. Strogatz, SIAM J. Appl. Math. **50**, 1645 (1990).
[22] S. H. Strogatz, R. E. Mirollo, and P. C. Matthews, Phys. Rev. Lett. **68**, 2730 (1992).
[23] K. Wiesenfeld, Phys. Rev. A **44**, 3543 (1991).
[24] D. Dhar, Phys. Rev. Lett. **64**, 1613 (1990).
[25] See, e.g., K. Christensen and Zeev Olami, Phys. Rev. E **48**, 3361 (1993).
[26] G. Grinstein, J. Stat. Phys. **5**, 803 (1988).
[27] See, e.g., H. G. Schuster, *Deterministic Chaos* (Physik-Verlag, Weinheim, 1984).
[28] T. Bohr, G. Grinstein, Y. He, and C. Jayaprakash, Phys. Rev. Lett. **58**, 2155 (1987).
[29] See, e.g., Hao Bai-Lin, *Chaos II* (World Scientific, Singapore, 1990).
[30] Y. C. Zhang, Phys. Rev. Lett. **63**, 470 (1989).
[31] I. M. Jánosi, Phys. Rev. A **42**, 769 (1990).
[32] J. Kertész and L. B. Kiss, J. Phys. A **23**, L433 (1990).
[33] In several cases, when low dimensional chaos is supposed to be found in a natural time series, authors did not consider the serious limitations of the applied methods arising from environmental noise and the small amount of available data. For related criticisms see, e.g., P. Grassberger, *ibid.* **323**, 609 (1986); I. Procaccia, Nature **333**, 498 (1988).

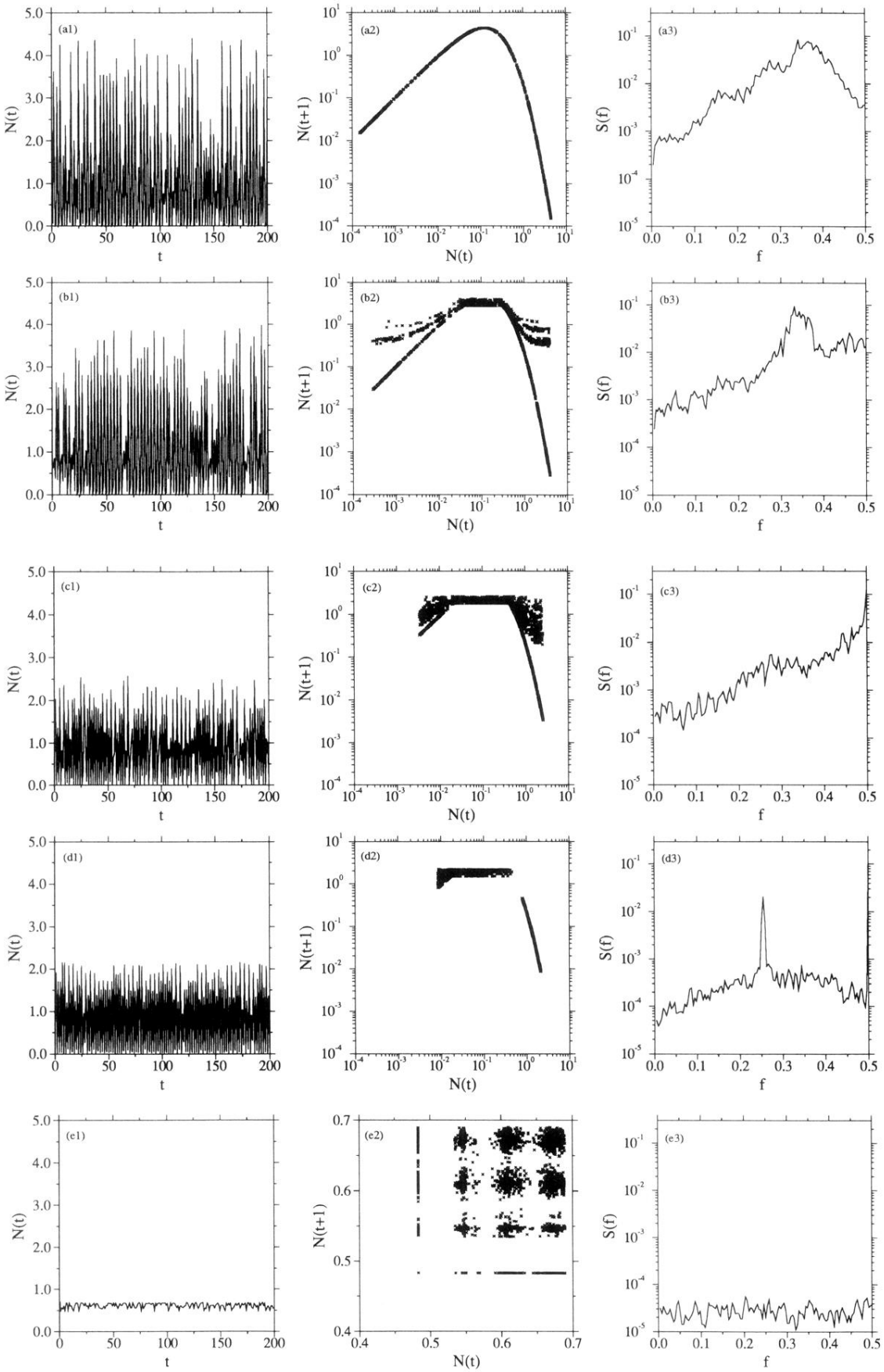

FIG. 1. Time series, first return maps, and power spectra of the population density N of a given site with varying threshold parameter. (a) No interaction ($k = \infty$), (b) $k = 4.0$, (c) $k = 2.69$, (d) $k = 2.165$, and (e) $k = 0.69$ (from top to bottom).

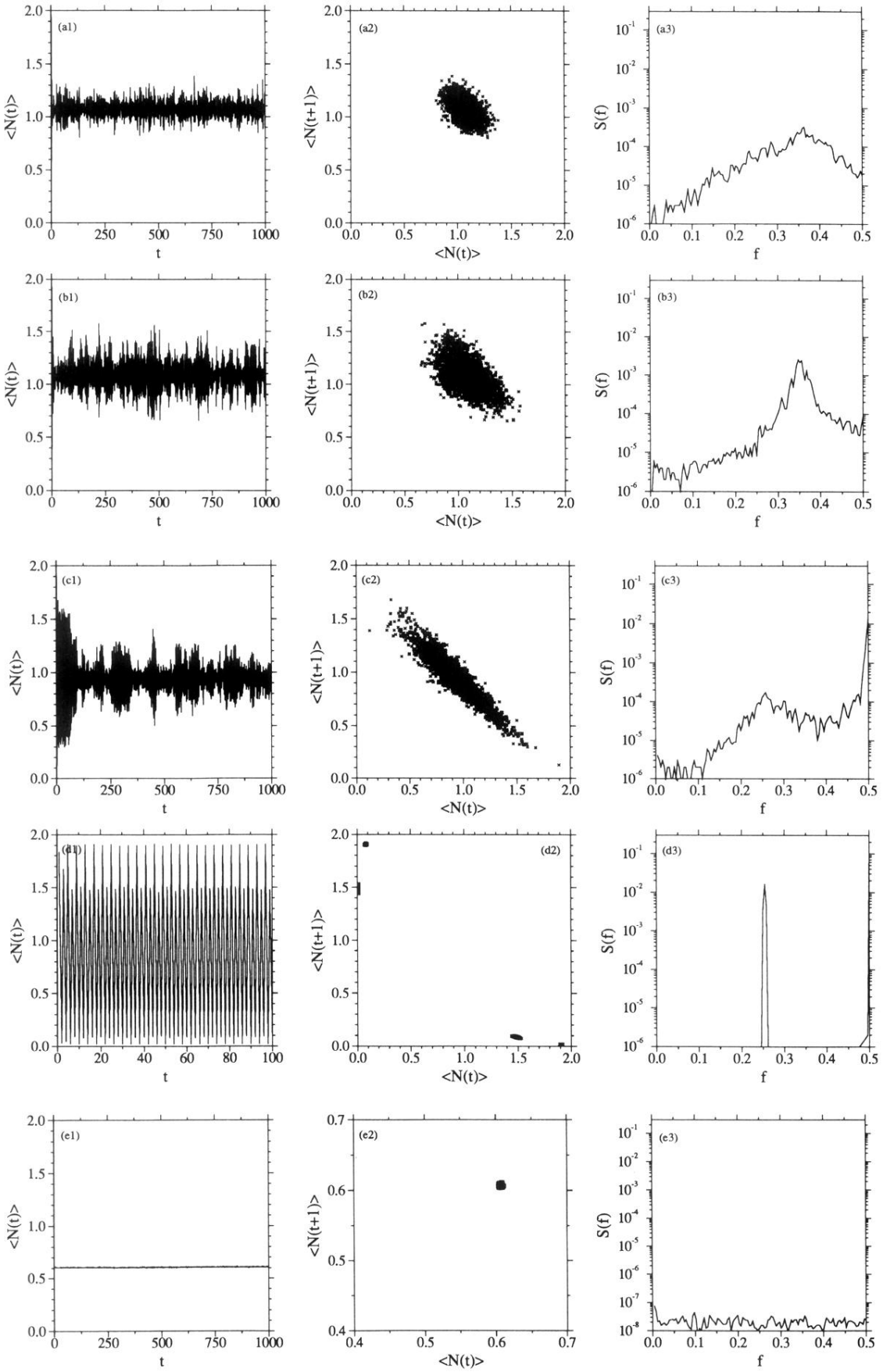

FIG. 2. Time series, first return maps, and power spectra of the metapopulation density [Eq. (5)] with varying threshold parameter. (a) No interaction ($k = \infty$), (b) $k = 4.0$, (c) $k = 2.69$, (d) $k = 2.165$, and (e) $k = 0.69$ (from top to bottom).

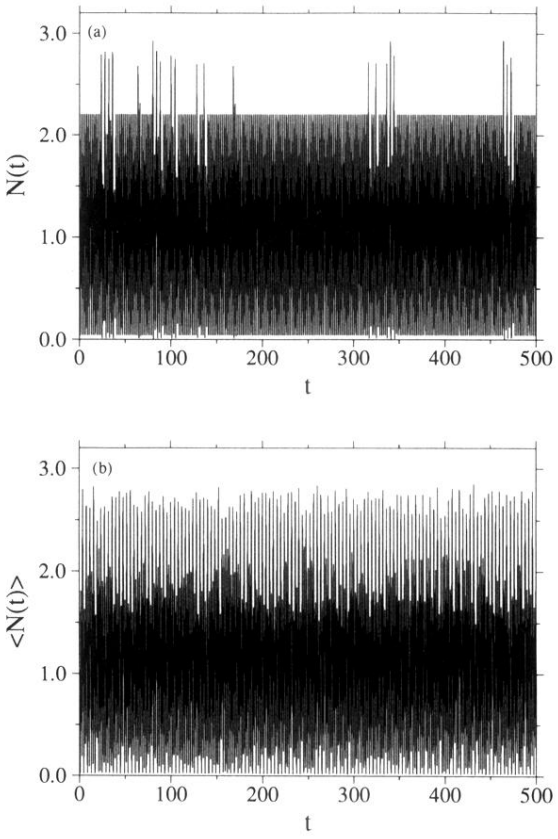

FIG. 8. Time series of (a) the central site and (b) the lattice average for the same parameters as in Fig. 7.